

Examining the role of red background in magnocellular contribution to face perception

Bhuvanesh Awasthi, Mark A Williams, Jason Friedman

This study examines the role of the magnocellular system in the early stages of face perception, in particular sex categorization. Utilizing the specific property of magnocellular suppression in red light, we investigated visually guided reaching to low and high spatial frequency hybrid faces against red and grey backgrounds. The arm movement curvature measure shows that reduced response of the magnocellular pathway interferes with the low spatial frequency component of face perception. This is the first definitive behavioral evidence for magnocellular contribution to face perception.

1
2 Examining the role of red background in magnocellular contribution to face
3 perception
4
5
6
7
8
9

10 Bhuvanesh Awasthi¹ *, Mark A Williams², Jason Friedman³
11
12
13
14
15

16 ¹Centre for Cognition and Decision Making, National Research University Higher School of
17 Economics. Moscow, Russia
18

19 ²Department of Cognitive Science, ARC Centre of Excellence in Cognition and its Disorders,
20 Macquarie University, Sydney, Australia
21

22 ³Department of Physical Therapy, Tel Aviv University, Tel Aviv, Israel
23
24
25
26
27
28
29
30
31
32
33
34

35 *Correspondence: Bhuvanesh Awasthi, Centre for Cognition and Decision Making, National
36 Research University Higher School of Economics. Moscow, Russia
37
38

39 E-mail: bhuvanesh.awasthi@gmail.com
40
41

42 Examining the role of red background in magnocellular contribution to face
43 perception

44
45
46

47 This study examines the role of the magnocellular system in the early stages of face perception,
48 in particular sex categorization. Utilizing the specific property of magnocellular suppression in
49 red light, we investigated visually guided reaching to low and high spatial frequency hybrid faces
50 against red and grey backgrounds.

51

52 The arm movement curvature measure shows that reduced response of the magnocellular
53 pathway interferes with the low spatial frequency component of face perception. This is the first
54 definitive behavioral evidence for magnocellular contribution to face perception.

55

56 Keywords: magnocellular pathway, spatial frequency, face perception, reach trajectories

57

58 1.0 Introduction

59 Perception of biologically relevant information from the environment is an essential
60 feature of the primate sensory system. Humans are efficient and quick in detecting briefly
61 viewed biological visual stimuli, in particular, faces. In contrast to non-face objects, face
62 perception is known to be carried out in a more configural manner, i.e, the information from the
63 face is processed as an undifferentiated whole, at a single glance, beyond just the sum of the
64 parts or the interrelations of the parts (Young, Hellawell & Hay, 1987; Tanaka & Farah, 1993;
65 Maurer, Le Grand, & Mondloch, 2002).

66

67 Different aspects of facial information processing have been associated with distinct
68 ranges of spatial frequencies. For instance, configural processing may stem from low level
69 sensory and perception mechanisms, particularly through low spatial frequency (LSF)
70 information, whereas high spatial frequency (HSF) conveys more local featural information
71 about the stimulus (Shulman, Sullivan, Gish & Sakoda, 1986; Hughes, Nozawa, & Kitterle,
72 1996; Han, Yund & Woods, 2001). The coarse-scale blurred features of LSF image may capture
73 the diagnostic information needed for configural processing while fine-tuned details through
74 HSF facilitates information regarding finer details of the stimuli.

75

76 Research on spatial frequency and visual processing has also established that LSF
77 information is carried mainly via magnocellular channels that are structured for faster
78 transduction of visual signals to the subcortical and cortical regions (Livingstone & Hubel, 1988;
79 Merigan & Maunsell, 1993; Bar, 2003). Fine-grained high spatial frequency (HSF) information,
80 on the other hand, has a comparatively slower transmission via the parvocellular channels

81 (Livingstone & Hubel, 1988; Bullier, 2001). Magnocellular neurons project predominantly to the
82 dorsal visual stream for information regarding motion and spatial location, while the recognition
83 of object identity is processed along the ventral cortical pathway, mainly subserved by
84 parvocellular channels (Felleman & Van Essen, 1991; Orban, Van Essen & Vanduffel, 2004).
85 Finer details regarding the object's color, shape, inner feature and textures are carried chiefly
86 through the slower parvocellular system, while the magnocellular system carries achromatic and
87 global shape information (Kaplan & Shapley, 1986; Macé, Thorpe & Fabre-Thorpe, 2005).
88 Parvo-outputs are thus predominant at higher spatial frequencies while Magno-outputs dominate
89 at low spatial frequencies (Tobimatsu, Tomoda & Kato, 1995).

90

91 The magnocellular system facilitates rapid detection of object identity and location
92 despite poor spatial resolution. Research findings illustrate that top-down modulations
93 (predominantly through the LSF channels) bias the output of the bottom-up sensory input
94 thereby facilitating rapid global processing (Kveraga, Boshyan & Bar, 2007; Kveraga, Ghuman
95 & Bar, 2007). The global predictions obtained from the blurred LSF image are then
96 progressively integrated with the HSF information in subsequent processes along the inferior
97 temporal regions of the cortex. This reduces the computational demands on the system and
98 improves efficient recognition.

99

100 Laycock, Crewther and Crewther (2007) have proposed a 'magnocellular advantage'
101 model of visual perception wherein an initial rapid feedforward sweep through the dorsal stream
102 activates parietal and frontal areas that further feeds back into the primary visual cortex.

103 However, despite several neuroimaging and neurophysiology reports, direct evidence for the role
104 of the magnocellular system in the early stages of face perception remains to be established.

105

106 Here, to examine the magnocellular contribution to face perception, we used a simple
107 technique to selectively suppress the magnocellular system. We exploited the property of the
108 magnocellular pathway's inhibitory response to red light (due to the long wavelength of red
109 light). Early on, Wiesel and Hubel (1966) reported inhibition of magnocellular channels by red
110 light, followed by several other research reports in recent times (Okubo & Nicholls, 2005;
111 Bedwell, Miller, Brown, Yanasak, 2006; West, Anderson, Bedwell & Pratt, 2010). Red light
112 causes tonic suppression of the excitatory activity of (type IV) cells of the magnocellular
113 pathway. This specific property of magnocellular suppression due to red color has been
114 demonstrated in both animal and human studies throughout the visual stream including the
115 retinal ganglion cells (de Monasterio, 1978), the lateral geniculate nucleus (Dreher, Fukada,
116 Rodieck, 1976) and the striate cortex (Livingstone & Hubel, 1984). Human behavioral studies
117 have reported reduced performance on magnocellular pathway-dependent tasks in the presence
118 of a red background (Breitmeyer & Breier, 1994; Chapman, Hoag & Giaschi, 2004; Bedwell,
119 Brown & Orem, 2008) on a variety of tasks such as reading performance (Chase, Ashourzadeh,
120 Kelly, Monfette & Kinsey, 2003), depth perception (Brown & Koch, 2000) and global motion
121 (Breitmeyer & Williams, 1990). An fMRI study reported decreased activity in the V5/MT region
122 (that receives substantial magnocellular input) with red as opposed to a neutral background
123 (Bedwell, Miller, Brown & Yanasak, 2006).

124

125 By manipulating the background color, we designed the study to examine the
126 contribution of the magnocellular pathway when processing LSF-HSF face hybrids. In the
127 experimental task (described in detail in the methods section), there is greater emphasis on M-
128 pathway input (i.e., identifying location, whether left or right) of the target rather than mere
129 identification. Since the LSF interference is reliant on adequate magnocellular pathway
130 functioning and the color red suppresses such functioning, we hypothesize that the LSF
131 component will have less effect on the trajectories with a red background compared to a grey
132 one.

133

134 In addition, to maximize the difference between the LSF and HSF components of the
135 LSF-HSF face hybrids, we shall present the stimuli at foveal and peripheral locations. The
136 density distribution of magnocellular channels is known to be much higher at periphery (Silveira
137 & Perry, 1991) and so it is likely that LSF interference at peripheral locations (see Awasthi,
138 Friedman & Williams, 2011a for more details) can help tease apart the differential engagement
139 of the two channels. Since we hypothesize that red light shall impair magnocellular functioning,
140 the effect on trajectories is likely to be less pronounced at peripheral locations with a red
141 background compared to a grey one.

142

143 We use a relatively novel behavioral measure that provides rich information regarding
144 perceptual decision making in real-time. Recent research reports (Gold & Shadlen, 2001; Spivey
145 & Dale, 2006; Freeman & Ambady, 2011) have demonstrated that motor responses are generated
146 in parallel with partial (incomplete) perceptual information that is continuously updated by
147 perceptual-cognitive processing over time. Continuous tracking of hand movements during the

148 reaching task can reveal otherwise hidden, underlying parallel processes in real- time (Song &
149 Nakayama, 2009). Tracking of hand movements are reported to provide unusually high-fidelity,
150 real-time access to fine-grained traces of the perceptual phenomena that are otherwise not
151 captured by discrete traditional measures (Resulaj, Kiani, Wolpert & Shadlen, 2009). Using a
152 discrete measure (such as a button press reaction time response), we cannot disentangle with
153 certainty and precision the early versus late processing of LSF and HSF in responding to the
154 hybrids. Analyzing the shapes of the trajectories and separating the early versus late components
155 of reaching movements allow early access to the state of the decision making process while the
156 subjects reach to the targets.

157

158 There is a growing body of research that models how manual action exposes the real-time
159 unfolding of underlying cognitive processing (Song & Nakayama, 2009; Resulaj et al 2009). In
160 our study, the reaching trajectories can potentially tease apart magno versus parvo inputs because
161 in addition to the top-down recognition (of pointing to the target sex), the subjects are required to
162 identify the location of target (whether left or right). In doing so, the trajectory they take (as the
163 information in hybrids progressively unfolds) provides a window into the magnocellular
164 afferents that project onto the dorsal stream structures important for reaching. Amongst a wide
165 variety of measures that are used to examine the trajectories of movement (Awasthi, 2012), we
166 use path offset/curvature area and movement onset times in this study as these are well suited to
167 provide valuable information based on task requirements and study design.

168

169

170 **2.0 Method**

171

172 **2.1 Ethics Statement**

173 The ethical aspects of this study were approved by the Human Research Ethics Committee
174 (HREC) of Macquarie University.

175

176 **2.2 Stimuli, Design and Procedure**

177 Similar to the previous experiments (described in Awasthi, Friedman & Williams, 2011a;
178 2011b), male and female face images were Fourier transformed and multiplied by low-pass and
179 high-pass Gaussian filters to preserve low (<8 cpf) and high SF (>25 cpf) information in each
180 image. The images were equated for luminance and contrast energy using Shine toolbox before
181 filtering and were then superimposed to make LSF-HSF hybrid images (see Figure 1). Both the
182 grey (RGB values of 75, 75, 75) and red background (RGB values of 255, 0, 0) had equal
183 luminance. Presentation software (Neurobehavioral Systems) was used to present the stimuli.
184 The stimuli had a mean height and width of 5.7° visual angle at foveal presentation and were
185 presented 21.7° from fixation for peripheral presentation.

186

187 Four combinations of hybrid images were used in the experiment. A four-factor within-
188 subjects design was used, the factors being Eccentricity (periphery, fovea), Target Location (left,
189 right), Target Congruity (congruent, incongruent) and Distractor Conflict (present, absent). All
190 factors were fully crossed, yielding sixteen experimental conditions. Congruity was defined as
191 the sex of the HSF face being the same as that of the LSF face in a hybrid. Thus, MM and FF
192 were congruent whereas FM and MF were incongruent conditions. For instance, in the hybrid
193 image **FF**, the first letter (**F**) of the hybrid indicates the sex of the LSF face (**F**emale) and the

194 second letter (**F**) indicates the sex of the HSF face (**F**). For hybrid **FM**, the LSF face is **F**emale
195 and the HSF face is **M**ale (Figure 1a).

196

197 (Insert Figure 1 somewhere here)

198

199 For each subject, the target sex was assigned at the beginning of the experiment for the
200 entire session (e.g., Female). The task involved pointing to the target (e.g., female face) on the
201 touch screen. At viewing distance, the HSF face was salient (most visible) and was the target for
202 all trials throughout the experiment. In congruent target trials, both the LSF and HSF
203 components of the hybrid face were the same sex (e.g., both Female; FF) while for the
204 incongruent target trials, the LSF component was of the opposite sex (e.g., Male; MF). To
205 maximize the LSF interference effect, we also manipulated whether the face on the other side of
206 the target location held a target-matched LSF distractor (e.g., an LSF female) or not (e.g., no LSF
207 female). There was no HSF distractor. Two hybrid faces were presented at the left and right side
208 of the fixation cross (for foveal presentation) and at far periphery (for peripheral presentation)
209 (Figure 1b). Subjects were instructed to begin the task with eyes on the fixation. After the initial
210 liftoff, they could move their eyes freely.

211

212 **2.3 Subjects**

213 Right-handed subjects were recruited from the Macquarie University community who
214 volunteered their participation. All subjects reported normal or corrected-to-normal vision and
215 gave written, informed consent before participation. 15 subjects (seven females, mean age: 25.2
216 years, SD=4.3) participated in the task.

217 2.4 Procedure

218 Subjects sat in a quiet, dark room at a table with a LCD touch screen (70 × 39 cm, 1360 ×
219 768 pixels, 60Hz) positioned approximately 70 cm in front of them. Two small infrared light
220 emitting diode (LED) markers were attached to the right index fingertip of the subject. The
221 starting position (a button) was aligned with the body midline, approximately 20 cm in front of
222 the subjects. Each trial began with subjects placing their right index finger on the centrally
223 located starting button in front of the touchscreen. Hand movements were tracked with an
224 Optotrak Certus Motion Capture System (Northern Digital Inc.) at a 200 Hz sampling rate. The
225 tracking system was calibrated at the beginning of each experiment.

226

227 In both the grey background and the red background conditions, two hybrids were
228 presented *peripherally* and *centrally* in alternate blocks. The peripheral and central presentation
229 of hybrids is equivalent in terms of stimuli and the procedure, except that in the central
230 condition, two hybrids were present on either side of fixation. Subjects performed the red and
231 grey sessions on consecutive days in a counterbalanced manner. They were assigned Male or
232 Female as the target sex (also counter-balanced across subjects). They were instructed to
233 maintain fixation on a cross at the center of the screen (that appeared for 1000 ms) before
234 reaching out and pointing to the target. Subjects had to begin their reaching response within 350
235 ms of target onset but their final responses (either left or right) were not speeded, with sufficient
236 (cutoff 1.5 seconds) time for the finger to change direction or correct its course. Trials were
237 aborted when started too early (before the target onset) or too late (after 350 ms). For all
238 responses, feedback was provided onscreen. After a block of training with 40 trials, 16 blocks of
239 40 trials each were carried out with adequate breaks in between. Only the correct response trials

240 were used for further data analysis. The subjects had a mean accuracy rate of 93.34 % (SD=3.69)
241 for the grey background and 94.11% (SD=3.21) for the red background.

242

243 We used cubic splines for data smoothing and interpolation when markers were occluded
244 (for less than 10% of the trajectory in a trial). Movement data was analyzed using Matlab (The
245 Mathworks, Inc). We calculated the maximum deviation from a straight-line path from start to
246 end of the movements. We then defined maximum curvature as the ratio of this deviation to the
247 length of the straight-line path (Atkeson & Hollerbach, 1985; Smit & Van Gisbergen, 1990). The
248 average maximum curvature was computed for all subjects and used as the dependent variable.

249

250 **2.5 Curvature Results**

251 The curvature in the trajectory is taken as a measure of uncertainty in the decision
252 making process. The mean trajectories (pooled for all subjects) are shown in Figure 2. The
253 differences in the trajectories were initially quantified by comparing the maximum curvature.
254 When subjects select a target and do not change their mind (i.e., when the LSF and HSF
255 components unambiguously correspond to one target), they reach directly to the target, and the
256 curvature is low. When there are competing sources of information (i.e., the LSF and HSF are
257 incongruent, or there is an LSF distractor on the other side), this uncertainty in the decision
258 making process is reflected through greater curvature. Repeated measures ANOVA with
259 background color (grey, red), eccentricity (periphery, fovea), target congruity (congruent,
260 incongruent), distractor conflict (present, absent) and target location (left, right) was carried out.

261 (Insert Figure 2 somewhere here)

262

263 Eccentricity, target congruity, distractor conflict and target location significantly
264 influenced the curvature as shown by the significant main effect of eccentricity $F(1, 14) = 5.00$,
265 $p < 0.05$, target congruity $F(1, 14) = 199.50$, $p < 0.001$, distractor conflict $F(1, 14) = 70.92$,
266 $p < 0.001$, and location $F(1, 14) = 14.73$, $p < 0.001$. The main effect of background color also
267 approached significance $F(1, 14) = 4.56$, $p = 0.051$ with pairwise comparisons showing larger
268 curvature for grey (mean=0.283) than red (mean=0.237) background.

269

270 Mean curvature across eccentricity was significantly larger in red background conditions
271 than in the grey background conditions as shown by a significant interaction between
272 background color and eccentricity $F(1, 14) = 5.00$, $p = 0.042$. Post-hoc (Tukey HSD) analysis
273 showed that difference between peripheral and foveal presentations were significantly greater in
274 red ($M = 0.2$) than at the grey ($M = 0$) background at $p < 0.01$.

275

276 Mean curvature due to target congruity was significantly larger in peripheral
277 presentations ($M = 0.22$) than in the foveal presentations ($M = 0.30$) as shown by a significant
278 interaction between eccentricity and target congruity $F(1, 14) = 14.24$, $p = 0.002$. Post-hoc
279 (Tukey HSD) analysis showed that target congruity differences were significantly larger at
280 periphery (0.08) than at the fovea (0.06) at $p < 0.001$. Further results show that congruity
281 differences at fovea for grey background ($M = 0.27$) were significantly larger than for the red
282 background ($M = 0.20$) but not for the periphery, shown by a three-way interaction between
283 background color X eccentricity X target congruity $F(1, 14) = 14.24$, $p = 0.002$. Post-hoc (Tukey
284 HSD) analysis showed that target congruity differences at fovea were significantly larger for
285 grey (mean difference= 0.06; $p < 0.01$) than for red background. Tests of violations of sphericity

286 were performed on the data.

287

288 **4.0 Discussion**

289

290 In this study, we examined the role of LSF and HSF in a face categorization task at fovea

291 and periphery. To infer the role of the magnocellular visual pathway, a novel technique was used

292 wherein the reaching performance against a red background (believed to suppress the

293 magnocellular pathway) was compared to that against a neutral grey background. Results from

294 curvature measure demonstrate the differential role of grey and red background in sex

295 categorization task, likely indicating the magnocellular suppression. Previous research has

296 implicated the possible role of the magnocellular pathway in rapid detection and categorization

297 of achromatic stimuli (Delorme, Richard & Fabre-Thorpe, 1999). For example, Michimata,

298 Okubo and Mugishima (1999) showed that red background impairs the perception of a global

299 visual pattern believed to rely on LSF processing. Other studies have also shown reduced flicker

300 sensitivity when presented on a red background (Stromeyer, Cole & Kronauer, 1987). West,

301 Anderson, Bedwell and Pratt (2010) also demonstrated that the perception of fearful faces is

302 suppressed under red diffused light, lending support to the idea of global precedence through the

303 magnocellular pathway.

304

305 Early information in LSF faces is carried through the magnocellular pathway and this

306 information may be crucial for quick start times required in the fast categorization task used here.

307 Spatial frequency and stimulus location (peripheral versus foveal presentation) significantly

308 influence the categorization task as shown in the curvature measure.

309

310 Skottun (2004) has argued that red light also attenuates the parvocellular red–green color-
311 opponent cells. In contrast, studies have demonstrated that color-contrast detection by red-green
312 opponent cones is confined to foveal vision and is known to fall steeply across the periphery
313 (Mullen & Kingdom, 2002; Mullen, Sakurai & Chu, 2005). It is probable that the red
314 background interacts with the parvocellular pathway as well, mechanisms of which remain to be
315 investigated.

316

317 Across all the red diffuse light literature, there is no standard measure of luminance;
318 instead there is a standard of keeping equiluminance across all conditions. It may be the case that
319 researchers who use high luminance may see a greater effect of inhibition of the M-pathway than
320 those who use lower luminance. However, researchers have been able to find the effects of red
321 diffuse light with both high luminance (Chapman, Hoag & Giaschi, 2004), and low luminance
322 (Mullen, Kingdom, 2002). Research by Breitmeyer has shown that dark adaptation was useful to
323 observe the inhibitory effects of red diffuse light (Breitmeyer & Breier, 1994; Breitmeyer &
324 Williams, 1990) by providing the required bias towards the M-pathway.

325

326 In our previous studies using the same experimental setup (Awasthi et al 2011a; b), we
327 demonstrated significantly larger peripheral interference by LSF information while reaching for
328 HSF targets. In concordance with our previous findings and the research showing higher density
329 distribution of magnocellular channels at periphery, the LSF interference in the current study
330 reflects the differential engagement of the magnocellular pathway in grey versus red background.
331 In yet another study using red glasses for experimental manipulation, Williams, Grierson and

332 Carnahan (2011) demonstrated that diffused red light suppresses magnocellular activity thereby
333 significantly disrupting visual threat processing.

334

335 Deficits in global identification of faces (as seen in prosopagnosia) and other
336 developmental conditions might have a magnocellular contribution (Grinter, Maybery &
337 Badcock, 2010). It is likely that magnocellular dysfunction, if present in face recognition
338 deficits, concerns more integrated processes at levels where information from parvocellular and
339 magnocellular channels interact. In line with Laycock et al.'s magnocellular deficit proposal, we
340 recently reported delayed integration of low and high spatial frequency information in
341 developmental prosopagnosia (Awasthi et al 2012). This integration failure could be due to an
342 attention-perception mechanism that favors parvocellular over magnocellular channels reflecting
343 a tradeoff between segregation and integration of information (Yeshurun, 2004) that ultimately
344 reflects in impaired face processing. The deficient responsiveness of the magnocellular channels
345 has been reported in schizophrenia (Martinez et al., 2008) as well as in other developmental
346 conditions (Laycock et al., 2007), subsequently influencing higher level perceptual processing.

347

348 Findings from our study provide strong support for the role of the magnocellular pathway
349 in face perception. The contextual associations between stimuli in the environment activate
350 predictive early guesses, available through partial, blurred, yet rapidly available information
351 about the stimulus identity. It is noteworthy though that non-face object may also utilize this
352 magnocellular advantage. However, much experimental data on the topic remains to be
353 generated to generalize the advantage to certain or all object classes. Fenske, Aminoff, Gronau
354 and Bar (2006) demonstrate the top- down facilitation that is triggered by both the early

355 information about an object, as well as by contextual associations between an object and other
356 objects in the vicinity within which it is typically recognized. As the magnocellular pathway is
357 predominantly attuned to low spatial frequency (LSF) information, Bar's proposed model
358 predicts that the early, quick and dirty LSF information processing is projected to the orbito-
359 frontal cortex, which in turn selects potential matches based on the global, LSF-based properties
360 of the bottom-up input. Predictions to identity fine-tuned features of the stimulus global
361 properties (obtained initially from the blurred LSF image) are then projected to the high spatial
362 frequency dominated object recognition areas along the inferior temporal regions of the cortex. A
363 rapid projection via the magnocellular pathway plays a crucial role in this facilitation, resulting
364 in rapid recognition of biologically salient stimuli such as faces. Taken together, it may be more
365 appropriate to describe the predictions generated by the low and high SF as phases evolving over
366 time, rather than as separate bouts of visual information (although using separate pathways) each
367 one adding further to the perceptual processing. The magnocellular system helps in deciphering
368 the overall three-dimensional organization, position and movement of visual objects in the
369 environment. Selective engagement of the magnocellular system provides a framework for
370 expedient prioritization of biologically salient stimuli that compete for attention and action.
371

372 Figure legends

373

374 **Figure 1** (a) Stimuli: LSF-HSF hybrid images used in the experiments. To see the LSF content,
375 squint, blink, or step back from the figure (b) Experimental setup showing the touchscreen where
376 two hybrid images were presented peripherally and centrally in alternate blocks. Subjects start
377 each trial at the grey button on the table to reach out and touch the respective black target box on
378 the screen.

379

380 **Figure 2** (a) Mean trajectories for grey background (b) Mean trajectories for red background.

381

382

383

384

385

386

387

388

389

References

390

1. Atkeson CG, Hollerbach JM (1985) Kinematic features of unrestrained vertical arm

391

movements. *Journal of Neuroscience* 5(9): 2318-30.

392

2. Awasthi B (2012) An investigation into visually guided reaching to low spatial frequency

393

faces. PhD thesis, Macquarie University, available:

394

<http://trove.nla.gov.au/work/183902617?selectedversion=NBD51856861> accessed on

395

June 27, 2015.

396

3. Awasthi B, Friedman J, Williams MA (2011a) Processing of low spatial frequency faces

397

at periphery in choice reaching tasks. *Neuropsychologia* 49(7): 2136– 2141.

398

4. Awasthi B, Friedman J, Williams MA (2011b) Faster, stronger, lateralised: LSF support

399

for face processing. *Neuropsychologia* 49(13): 3583–3590.

400

5. Awasthi B, Friedman J, Williams MA (2012) Reach trajectories reveal delayed

401

processing of low spatial frequency faces in developmental prosopagnosia. *Cognitive*

402

Neuroscience 3(2): 120-130.

403

6. Bar M (2003) A cortical mechanism for triggering top-down facilitation in visual object

404

recognition. *Journal of Cognitive Neuroscience* 15: 600–609.

405

7. Bedwell JS, Brown JM, Orem JM (2008) The effect of a red background on location

406

backward masking by structure. *Perception and Psychophysics* 70 (3): 503–507.

407

8. Bedwell JS, Miller LS, Brown JM, Yanasak NE (2006) Schizophrenia and red light:

408

fMRI evidence for a novel biobehavioral marker. *International Journal of Neuroscience*

409

116: 881–894.

- 410 9. Bedwell JS, Miller LS, Brown JM, Yanasak NE (2006) Schizophrenia and red light:
411 fMRI evidence for a novel biobehavioral marker. *International Journal of Neuroscience*
412 116: 881–894.
- 413 10. Breitmeyer BG, Breier JI (1994) Effects of background color on reaction time to stimuli
414 varying in size and contrast: inferences about human M channels. *Vision Research* 34:
415 1039–1045.
- 416 11. Breitmeyer BG, Williams MC (1990) Effects of isoluminant- background color on
417 metacontrast and stroboscopic motion: interactions between sustained (P) and transient
418 (M) channels. *Vision Research* 30: 1069–1075.
- 419 12. Brown JM, Koch C (2000) Influences of occlusion, color, and luminance on the
420 perception of fragmented pictures. *Perceptual and Motor Skills* 90: 1033–1044.
- 421 13. Bullier J (2001) Integrated model of visual processing. *Brain Research Review* 36: 96-
422 107.
- 423 14. Chapman C, Hoag R, Giaschi D (2004) The effect of disrupting the human magnocellular
424 pathway on global motion perception. *Vision Research* 44: 2551–2557.
- 425 15. Chase C, Ashourzadeh A, Kelly C, Monfette S, Kinsey K (2003) Can the magnocellular
426 pathway read? Evidence from studies of color. *Vision Research* 43: 1211–1222.
- 427 16. de Monasterio FM (1978) Properties of concentrically organized X and Y ganglion cells
428 of macaque retina. *Journal of Neurophysiology* 41(6): 1394-1417.
- 429 17. Delorme A, Richard G, Fabre-Thorpe M (1999) Rapid processing of complex natural
430 scenes: A role for the magnocellular pathway. *Neurocomputing* 26–27: 663–670.

- 431 18. Dreher B, Fukada Y, Rodieck RW (1976) Identification, classification and anatomical
432 segregation of cells with x-like and y-like properties in the lateral geniculate nucleus of
433 old-world primates. *Journal of Physiology* 258(2): 433–452.
- 434 19. Felleman DJ, Van Essen DC (1991) Distributed hierarchical processing in the primate
435 cerebral cortex. *Cerebral Cortex* 1: 1–47.
- 436 20. Fenske MJ, Aminoff E, Gronau N, Bar M (2006) Top-down facilitation of visual object
437 recognition: Object-based and context-based contributions. *Progress in Brain Research*
438 155: 3-21.
- 439 21. Freeman JB, Ambady N (2011) Hand movements reveal the time-course of shape and
440 pigmentation processing in face categorization. *Psychonomic Bulletin & Review* 18: 705-
441 712.
- 442 22. Friedman J, Brown S, Finkbeiner M (2013) Linking cognitive and reaching trajectories
443 via intermittent movement control. *Journal of Mathematical Psychology* 57(3-4): 140-
444 151.
- 445 23. Gold JJ, & Shadlen MN (2001) Neural computations that underlie decisions about
446 sensory stimuli. *Trends in Cognitive Sciences* 5: 10-16.
- 447 24. Grinter EJ, Maybery MT, Badcock DR (2010) Vision in developmental disorders: Is
448 there a dorsal stream deficit? *Brain Research Bulletin* 82: 147-160.
- 449 25. Han S, Yund W, Woods WL (2001) An ERP study of the global precedence effect: the
450 role of spatial frequency. *Clinical neurophysiology* 114: 1850-1865.
- 451 26. Hughes HC, Nozawa G, Kitterle F (1996) Global precedence, spatial frequency channels,
452 and the statistics of natural images. *Journal of Cognitive Neuroscience* 8: 197-230.

- 453 27. Kaplan E, Shapley RM (1986) The primate retina contains two types of ganglion cells,
454 with high and low contrast sensitivity. *Proc Natl Acad Sci U S A* 83:2755–2757.
- 455 28. Kveraga K, Boshyan J, Bar M (2007) Magnocellular projections as the trigger of top-
456 down facilitation in recognition. *Journal of Neuroscience* 27(48): 13232–13240.
- 457 29. Kveraga K, Ghuman AS, Bar M (2007) Top-down predictions in the cognitive brain,
458 *Brain and Cognition* 65: 145–168.
- 459 30. Laycock R, Crewther SG, Crewther DP (2007) A role for the ‘magnocellular advantage’
460 in visual impairments in neurodevelopmental and psychiatric disorders. *Neuroscience and*
461 *Biobehavioural Reviews* 31: 363–376.
- 462 31. Livingstone MS, Hubel DH (1984) Anatomy and physiology of a color system in the
463 primate visual cortex. *Journal of Neuroscience* 4(1): 309–356.
- 464 32. Livingstone MS, Hubel DH (1988) Segregation of form, color, movement and depth:
465 Anatomy, physiology and perception. *Science* 240: 740–749.
- 466 33. Macé MJ, Thorpe SJ, Fabre-Thorpe M (2005) Rapid categorization of achromatic natural
467 scenes: how robust at very low contrasts? *Eur J Neurosci* 21:2007–2018.
- 468 34. Martinez A, Hillyard SA, Dias EC, Hagler DJ Jr, Butler PD, Guilfoyle DN, Jalbrzikowski
469 M, Silipo G & Javitt DC (2008) Magnocellular Pathway Impairment in Schizophrenia:
470 Evidence from Functional Magnetic Resonance Imaging. *The Journal of Neuroscience*
471 28(30): 7492–7500.
- 472 35. Maurer D, Le Grand R, Mondloch CJ (2002) The many faces of configural processing.
473 *Trends in Cognitive Sciences* 6: 255–260.
- 474 36. Merigan WH, Maunsell JHR (1993) How parallel are the primate visual pathways?
475 *Annual Review of Neuroscience* 16: 369 - 402.

- 476 37. Michimata C, Okubo M, Mugishima Y (1999) Effects of background color on the global
477 and local processing of hierarchically organized stimuli. *Journal of Cognitive*
478 *Neuroscience* 11: 1–8.
- 479 38. Mullen KT, Kingdom F (2002) Differential distributions of red-green and blue-yellow
480 cone opponency across the visual field. *Visual Neuroscience* 19: 109-118.
- 481 39. Mullen KT, Sakurai M, Chu M (2005) Does L/M cone opponency disappear in human
482 periphery? *Perception* 34: 951-959.
- 483 40. Okubo M, Nicholls MER (2005) Hemispheric asymmetry in temporal resolution:
484 Contribution of the magnocellular pathway. *Psychonomic Bulletin & Review* 12(4): 755-
485 759.
- 486 41. Orban GA, Van Essen D, Vanduffel W (2004) Comparative mapping of higher visual
487 areas in monkeys and humans. *Trends in Cognitive Science* 8: 315–324.
- 488 42. Resulaj A, Kiani R, Wolpert DM, Shadlen MN (2009) Changes of mind in decision-
489 making. *Nature* 461: 263–266.
- 490 43. Shulman GL, Sullivan MA, Gish K, Sakoda XJ (1986) The role of spatial frequency
491 channels in the perception of local and global structure. *Perception* 15: 259-279.
- 492 44. Silveira LC, Perry VH (1991) The topography of magnocellular projecting ganglion cells
493 (M-ganglion cells) in the primate retina. *Neuroscience* 40(1):217–237.
- 494 45. Skottun BC (2004) On the use of red stimuli to isolate magnocellular responses in
495 psychophysical experiments: a perspective. *Visual Neuroscience* 21: 63–68.
- 496 46. Smit AC, Van Gisbergen JA (1990) An analysis of curvature in fast and slow human
497 saccades. *Experimental Brain Research* 81(2): 335-45.

- 498 47. Song J-H, Nakayama K (2009) Hidden cognitive states revealed in choice reaching tasks.
499 Trends in Cognitive Sciences 13(8): 360-366.
- 500 48. Spivey MJ, Dale R (2006) Continuous temporal dynamics in real-time cognition. Current
501 Directions in Psychological Science 15: 207-211.
- 502 49. Stromeyer CF III, Cole GR, Kronauer RE (1987) Chromatic suppression of cone inputs
503 to the luminance flicker mechanism. Vision Research 27: 1113–1137.
- 504 50. Tanaka JW, Farah MJ (1993) Parts and wholes in face recognition. Quarterly Journal of
505 Experimental Psychology 46A: 225–245.
- 506 51. Tobimatsu S, Tomoda H, Kato M (1995) Parvocellular and magnocellular contributions
507 to visual evoked potentials in humans: stimulation with chromatic and achromatic
508 gratings and apparent motion. Journal of Neurological Science 134: 73-82.
- 509 52. West GL, Anderson AK, Bedwell JS, Pratt J (2010) Red diffuse light suppresses the
510 accelerated perception of fear. Psychological Science 21(7): 992–999.
- 511 53. Wiesel TN, Hubel DH (1966). Spatial Spatial and chromatic interactions in the lateral
512 geniculate body of the rhesus monkey. Journal of Neurophysiology 29: 1115-1156.
- 513 54. Williams C, Grierson L, Carnahan, H (2011) Colour-induced relationship between affect
514 and reaching kinematics during a goal-directe aiming task. Experimental Brain Research
515 212(4): 555-561.
- 516 55. Yeshurun Y (2004) Isoluminant stimuli and red background attenuate the effects of
517 transient spatial attention on temporal resolution. Vision Research 44: 1375–1387.
- 518 56. Young AW, Hellawell D, Hay DC (1987) Holistic information in face perception.
519 Perception 16: 747–759.
- 520

Figure 1 (on next page)

Figure 1

(a) Stimuli: LSF-HSF hybrid images used in the experiments. To see the LSF content, squint, blink, or step back from the figure (b) Experimental setup showing the touchscreen where two hybrid images were presented peripherally and centrally in alternate blocks. Subjects start each trial at the grey button on the table to reach out and touch the respective black target box on the screen.

a



LSF Female- HSF Female (**FF**)



LSF Male- HSF Male (**MM**)

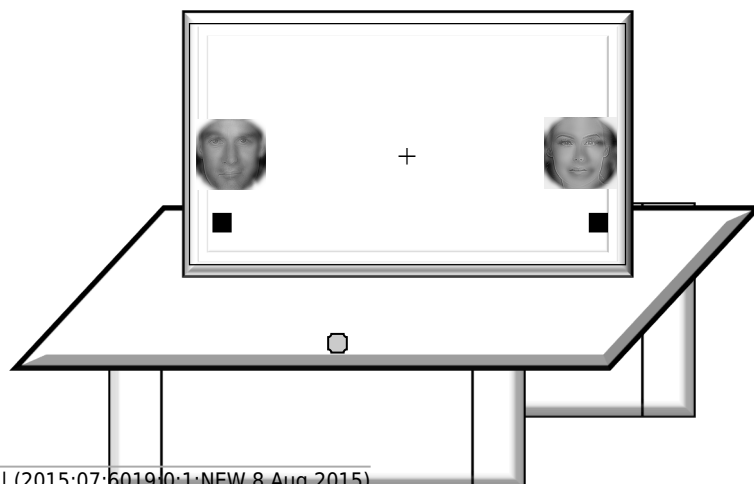


LSF Male- HSF Female (**MF**)



LSF Female- HSF Male (**FM**)

b



2

Figure 2

(a) Mean trajectories for grey background (b) Mean trajectories for red background.

